Revista Facultad de Ingeniería Universidad de Antioquia
ISSN: 0120-6230
revista.ingenieria@udea.edu.co
Universidad de Antioquia
Colombia

Botero, Maria Luisa; Molina, Alejandro
Simulation of the evaporation of drops from palm and castor oil biodiesels based on physical properties
Revista Facultad de Ingeniería Universidad de Antioquia, núm. 56, diciembre, 2010, pp. 40-48
Universidad de Antioquia
Medellín, Colombia

Simulation of the evaporation of drops from palm and castor oil biodiesels based on physical properties

Simulación de la evaporación de gotas de biodiesel de palma y ricino según sus propiedades físicas

Maria Luisa Botero, Alejandro Molina[*]

Bioprocesos y Flujos Reactivos, Facultad de Minas, Universidad Nacional de Colombia, Sede Medellín, Cr. 80. N.º 65-223. Medellín, Colombia

(Recibido el 13 de octubre de 2009. Aceptado el 10 de mayo de 2010)

Abstract

A reduction of oil reserves and an augmented production of greenhouse gases from fossil fuels have increased the use of biodiesel in internal combustion engines. Although physical and chemical properties of biodiesel and diesel are similar enough that allow the use of pure biodiesel in a traditional engine without considerable adjustments, differences in chemical structure of diesel and biodiesel change vaporization and combustion rates and can affect engine performance. In this study a model that can predict the evaporation rate of palm and castor oil biodiesel droplets at atmospheric pressure was developed. The model was validated with experimental data from the literature for the evaporation of n-heptane-droplets. The model estimates thermo-physical properties of biofuels using contribution group theory and was used to determine that castor oil biodiesel presents a lower evaporation rate than palm oil biodiesel due to differences in their physical properties (mainly density and vaporization enthalpy) which can be explained by a longer molecule and the presence of a hydroxyl groups in methyl ricinoleate, its main component.

----- *Keywords:* Diesel, biodiesel, heat transfer, droplet evaporation

Resumen

La disminución de reservas y la producción de gases efecto invernadero por parte de los combustibles fósiles han aumentado el uso de biodiesel en motores de combustión interna. Si bien las propiedades físico-químicas del biodiesel son lo suficientemente similares a las del diesel para permitir su uso puro en motores diesel sin necesidad de hacer ajustes de consideración en el

* Autor de correspondencia: teléfono: + 57 + 4 + 425 53 17, fax: + 57 + 4 + 234 10 02, correo electrónico: amolinao@unal.edu.co. (A. Molina)

motor, la diferente estructura química del diesel y biodiesel causa cambios en la velocidad de evaporación y combustión que pueden afectar el desempeño del motor. En este estudio se desarrolló un modelo que predice la velocidad de evaporación de gotas de biodiesel de palma y ricino a presión atmosférica el cual se validó con resultados experimentales de la evaporación de una gota de n-heptano obtenidos de la literatura. El modelo calcula las propiedades termo-físicas de los combustibles utilizando la teoría de contribución de grupos y predijo que el biodiesel de ricino presenta un tiempo de evaporación mayor que el de palma debido a diferencias en sus propiedades físicas como densidad y entalpía de vaporización las cuales se explican por la diferente composición química del biodiesel y los grupos funcionales presentes en sus alquil ésteres.

----- *Palabras clave:* Diesel, biodiesel, transferencia de calor, evaporación de gotas

Introduction

Vegetable oils are one of the most promising sources for renewable liquid fuels for diesel (in this paper diesel refers to the conventional fuel obtained from oil distillation) substitution. Biodiesel, a fuel obtained from the transesterification of vegetable oils, shows higher biodegradability, lubricity, and reduced toxicity and heat value when compared to diesel. Biodiesel does not contain sulfur, which is an additional environmental advantage [1, 2]

Although biodiesel and diesel show a similar behavior when supplied to an engine, both fuels have significant different chemical structure and as a consequence different physical properties such as density, viscosity, cloud point, cetane number and volatility. All these differences have subtle but noticeable effects on engine performance and pollutant emission [3, 4].

When a fuel droplet enters in a high temperature atmosphere, like a combustion chamber, the droplet is heated, evaporated, mixed and finally the fuel vapor burns, liberating energy for propulsion [5]. The evaporation of fuel droplets is the control mechanism in many combustion- engine applications [6]. The formation and homogeneity of the reactive mixture in diesel engines depends on the fuel evaporation characteristics [7].

Evaporation of fuel droplets has been a subject of interest for decades due to its importance in engineering applications. Along with experimental studies [8-11], an effort has been made to predict numerically the behavior of vaporizing droplets [12-16].

In the scientific literature, the prediction of the evaporation rate of droplets has been traditionally carried out according to the square diameter law (D^2 Law) [17]. This law simplifies the analysis of evaporation data and makes possible to understand the physical phenomena in the process. The simple formulation of D^2 law satisfactorily predicts key global parameters that characterize droplet evaporation and combustion, such as droplet evaporation rate and lifetime [18]. More complicated effects, not included in D^2 law, are: transient droplet heating, temperature gradient effects, recirculation inside the droplet, convection and thermal radiation. Contrary to the proliferation of multiple studies on evaporation of pure-fuel components, studies on the evaporation of diesel fuels are scarce and those for biodiesel were not found in the refereed literature.

In Colombia most of the vegetable oils commercialized for biodiesel production are from African palm. Biodiesel production from castor oil is as well a promising technology given its abundance in lands no suitable for food-production

agriculture. This article models the evaporation of isolated droplets of palm and castor biodiesel using the D^2 law at normal pressure. The model is validated with experimental results for n-heptane evaporation taken from [11]. The model has subroutines that predict the physical properties of fuels according to group-contribution theory. The aim of this investigation is not the modeling of droplet evaporation at engine conditions but the understanding of physical phenomena occurring during the evaporation of different fuels. The model shows that castor oil has a significant lower evaporation rate than palm oil. This result suggests that engines working with castor oil should have an advanced injection to improve mixture before combustion.

Model description

Figure 1a depicts the system to be modeled, considered as a spherical coordinate system. A droplet, of radius r_s and surface temperature T_s (assumed equal to the boiling point temperature, T_b), evaporates in a quiescent infinite atmosphere at temperature T_∞ (far away from droplet surface), due to the heat received from the hot atmosphere [19]. The vaporized fuel is transported to the atmosphere, by diffusion and Stefan convection [5] causing the shrinking of the droplet as time advances until complete evaporation ($r_s = 0$). A quasi-stationary process is assumed, given that the evaporation and transport rates of fuel are higher than the rate of droplet shrinkage.

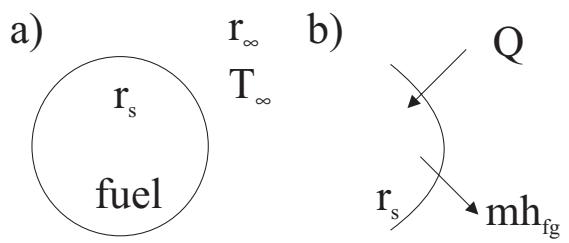

Figure 1 Energy balance in droplet surface. T_S: droplet surface temperature, T_b: boiling temperature. a) Temperatures in droplet, b) Detail of droplet/gas interface

Equation 1 and equation 2 show, according to the assumptions presented above, the mass and energy conservation expressions for the gaseous phase.

Mass conservation:

$$\dot{m} = 4\pi r^2 (\rho v_r) = \text{constant} \tag{1}$$

where ρ is the gas density in kg/m^3 and v_r is the bulk flow velocity in m^2/s

Energy conservation: Shvab-Zeldovich energy equation (assuming Lewis number equal to one):

$$\frac{d\left(r^2 \frac{dT}{dr}\right)}{dr} = \frac{\dot{m} c_{pg}}{4\pi k_g} \frac{dT}{dr} \tag{2}$$

Where c_{pg} is gas heat capacity in J/mol-K and k_g is gas thermal conductivity in W/m-K.

Solving equation 2 with the following boundary conditions: $T(r \to \infty) = T_\infty$ and $T(r = r_S) = T_b$ yields (equation 3) for the variation of temperature with radial distance in the gas phase

$$\frac{dT}{dr} = \frac{\dot{m} c_{pg}}{4\pi k_g r^2} \left[\frac{(T_\infty - T_b)\exp(-\dot{m} c_{pg} / 4\pi k_g r)}{1 - \exp(-\dot{m} c_{pg} / 4\pi k_g r)} \right] \tag{3}$$

Energy balance at the interface: The heat conducted from the gas to the interface is used to evaporate the liquid fuel (figure 1b):

$$4\pi k_g r_s^2 \left. \frac{dT}{dr} \right|_{r=rs} = \dot{m} h_{fg} \tag{4}$$

Where h_{fg} is the fuel latent heat of vaporization. With a final mass balance for the droplet and coupling equations 3 and 4 one obtains the D^2 law (Equation 5) that shows that the change in the square droplet diameter is constant and depends on fuel properties and the evaporation transfer number B [20].

$$\frac{dD^2}{dt} = -\frac{8 k_g}{\rho_d c_{pg}} \ln(B+1) \tag{5}$$

With $B = \frac{c_{pg}(T_\infty - T_b)}{h_{fg}}$

Where D and ρ_d are the drop diameter and density respectively.

Estimation of physical properties

According to the model described in Section 2, the prediction of droplet lifetimes in an evaporation process requires the knowledge of fuel properties such as density, thermal conductivity, enthalpy of vaporization and heat capacity. Since no data for these properties were found for castor and palm oil biodiesels, these properties were calculated based on their chemical composition and structure. The methodology used for properties estimation was validated with data by [21] for soybean biodiesel.

Biodiesel is a mixture of mono-alkyl esters in a proportion that depends on the raw material used in the fat transesterification process. Some of biodiesel properties can be traced to the structure of the fatty acid of which it is composed. Each ester component contributes to the properties of the biofuel [22]. Therefore, it is possible to estimate the properties of each pure component and then compute mixture properties based on some mixing rules. Table 1 shows chemical composition and some physical properties of typical castor and palm oil biodiesels as obtained from a commercial laboratory analyses. Data for density for POB was from reference [23]. Castor Oil Biodiesel (COB) is mainly composed by methyl ricinoleate (C18:1,OH) and, therefore, has the longest and most unsaturated hydrocarbon structure when compared to Palm Oil Biodiesel (POB). The later has a typical composition of 46% content methyl palmitate (C16:0), a slightly shorter chain with no unsaturation, and 37% content of methyl oleate (C18:1). Methyl linoleate (C18:2) is also a minor component of POB and COB.

Joback's group-contribution method was used to predict the critical properties of each methyl ester. From these values and some mixing rules, adequate correlations were used to estimate the physical properties of biofuels. Table 2 summarizes the different methods used to predict critical and other physical properties of the biofuels. All methods were taken from reference [24].

Table 1 Physical properties and composition of typical biodiesel

(Mass fraction)	*COB*	*POB*
C18:1,OH	0.93	0
C16:0	0	0.469
C18:0	0	0.037
C18:1	0.027	0.382
C18:2	0.043	0.112
Molecular weight	311.2807	284.1275
Final Boiling point (ºC)	357.5	302.16
Density at ref. temperature (kg/m^3)	0.9245 (20°C)	0.8644 (25°C)*

* From Ref. [21]

Table 2 Estimation methods

Property	*Method*
Critical properties	Method of Joback (1984;1987)
Density	Rackett equation (1970)
Latent heat of vaporization	Fish and Lielmezs method (1975), using Pitzer acentric factor (1995)
Heat capacity	Method of Joback (1984;1987)
Thermal conductivity	Chung method (1984;1988)
Mixing rules	Lee-Kesler equation

Results and analysis

Physical properties estimation

The physical properties of POB, COB and n-heptane were estimated according to the

procedure described above, n-heptane was included because it was used to validate the droplet evaporation model. The methods for estimation of density and latent heat of vaporization were validated against estimations carried out by [21] for Soybean Biodiesel. Our predictions were identical to those by [21] and are not presented due to space constrains.

At low temperatures (up to 100 ºC) the Rackett equation accurately predicts density as shown by [25] and also when compared to experimental data of POB obtained by [23]. According to [25], at higher temperatures (around 300ºC), close to biofuels boiling point, estimation deviates from experimental data within a range of 15-20%. In the simulation, density was calculated at the final boiling point of each fuel (see table 1 for COB and POB, the value for n-heptane was 98.3°C), and remained constant since droplet temperature was assumed to be constant (see Model Description). The predicted values of density at T_b were 710 kg/m^3, 645 kg/m^3 and 615 kg/m^3 for COB, POB and n-heptane respectively. COB presented the highest value of density, followed by POB and the lowest value was for n-heptane. This behavior is explained by the fact that COB has more intermolecular covalent bonds than the other fuels, given the larger chain size of its methyl esters [26]. POB has a lower density due to less unsaturations in methyl ester structures.

Figure 2 presents the estimated latent heat of vaporization at different temperatures. No experimental data were found in the refereed literature for this property, except for n-heptane at 298 K and 0.1 MPa which appears as a single data point in the figure and was accurately predicted. Vaporization enthalpy decreases when temperature increases and is zero at the critical temperature because liquid and gaseous phases do not coexist at this temperature. COB presented the highest vaporization enthalpy values followed by POB and then n-heptane which shows that chain size is a determinant factor in property estimation. Other important factors are the presence of the hydroxyl group in methyl ricinoleate (most significant component of COB) which influences the vaporization enthalpy because of the strong dipole-dipole bond [27] and the higher unsaturation degree than POB.

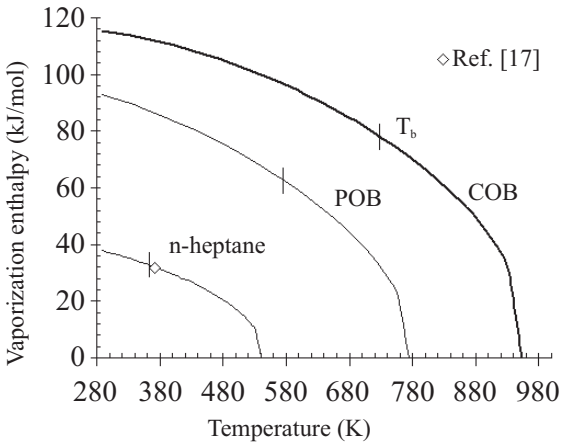

Figure 2 Predicted latent heat of vaporization vs. temperature. Plot shows one experimental point for n-heptane [19]. Short vertical lines show boiling temperature for each fuel

The predicted constant pressure heat capacity (c_p) for n-heptane in figure 3 is in good agreement with experimental data [28]. COB has the highest c_p at all temperatures evaluated. The c_p values for POB were similar to those of COB while those of n-heptane where the lowest. Because heat capacity increases with molecule size [26], it was expected that COB and POB present much higher heat capacity than n-heptane, and, given their similar molecular weights (see table 1) both have similar heat capacities. However, the value of c_p for COB is slightly higher than that for POB because of a higher number of atoms.

Predictions for thermal conductivity (figure 4) showed that n-heptane has the highest thermal conductivity. The order of thermal conductivity values (intermediate for POB and lowest for COB) is the result of the inverse proportionality of thermal conductivity with molecular mass and size [26].

This section showed that the model correctly predicts trends for the properties required for the D^2 law for the biodiesel in this study. Furthermore,

at some specific conditions where experimental data were available, the model perfectly agrees with these data. Model predictions are as well in agreement with the expected difference in properties for the three studied hydrocarbons.

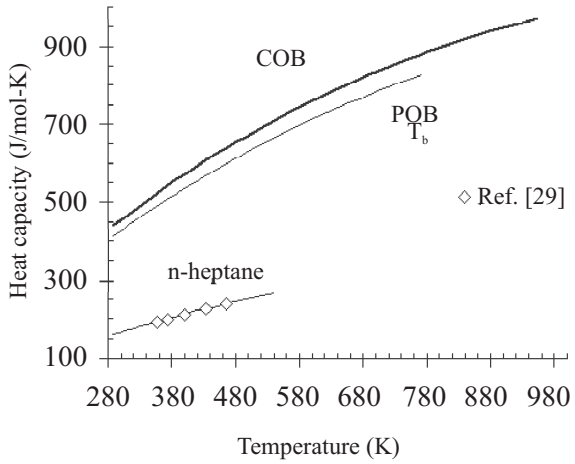

Figure 3 Predicted heat capacity vs. temperature. Experimental data of n-heptane [28] taken from [29]

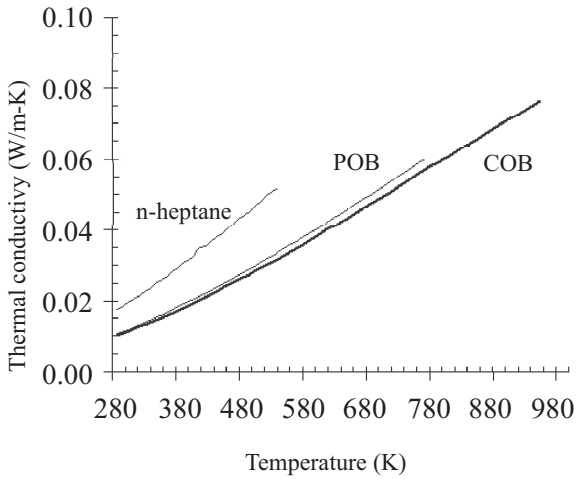

Figure 4 Predicted thermal conductivity vs. temperature

D^2 law for droplet evaporation

Validation

The model described in Section 2 was implemented using MATLAB. Results of experimental n-heptane droplet evaporation in microgravity obtained by [11] were used to validate the model. Although the data by [11] is for microgravity conditions, these data can be used to validate the model as the model does not consider the effect of the gravitational force.

In the experiments by [11], n-heptane droplets with initial diameter in the 0.6 mm - 0.8 mm were evaporated in a nitrogen atmosphere, at temperatures and pressures in the range of 400 K to 800 K and 0.1 MPa to 0.5 MPa, respectively.

From the data of [11] we modeled the experiments for a 0.7-mm diameter droplet at 0.1MPa. Fuel and ambient gas properties were calculated with the methods shown in Section 3 and with the open-source code CANTERA [30] and the NASA [31] database. Fuel vapor properties were estimated at atmosphere temperature, and fuel liquid properties at boiling temperature.

Figure 5 compares experimental data [11] with predictions by the model of normalized diameter vs. time divided by the squared of the initial diameter at 471 K, 555 K, 648 K and 741 K, the same temperatures evaluated by [11]. The value of the abscissa (time over the square of the initial diameter) is the same selected in ref. [11] and allows a simpler comparison of evaporation time for different drop diameters. For each temperature, in the first ~0.7 s mm^{-2} the droplet size slowly decreases as the initial heating of the droplet takes place. Once steady-state heating is obtained (for values higher than 0.7 s mm^{-2}), evaporation is faster and follows the D^2 law. This second part was the modeled. As figure 6 shows, at the highest temperatures (555 K, 648 K and 741 K) the model agrees with experimental data, but at 471 K, the model underestimates the evaporation rate as the experimental data seem to have two slopes.

A parity plot (figure 6) for predictions and experimental data of squared dimensionless diameter shows how at higher temperatures the model agrees with experimental data, but as temperature decreases, the difference between predictions and model increases, particularly as evaporation advances (smaller values of dimensionless

diameter). The reason for the discrepancy between model predictions and experimental data at low temperatures is unclear. One would expect an opposite trend if the reason for this difference could be explained by the droplet not achieving constant temperature during the heating up process. We are currently looking for more experimental data to test our model and have some insight that can explain this anomalous behavior at these conditions. However, most practical applications occur at high temperature range where the model agrees with experimental data.

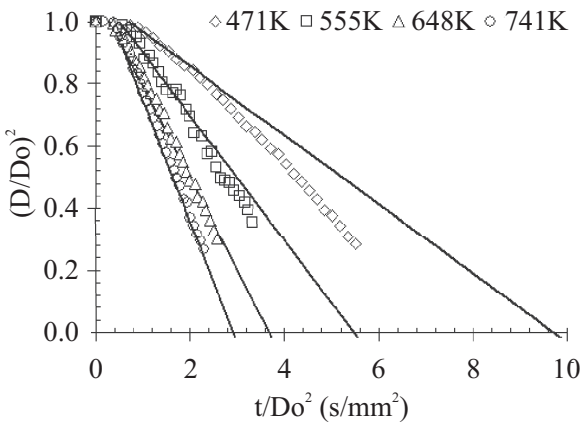

Figure 5 Variation of squared dimensionless droplet diameter with time divided by squared initial diameter (n-heptane, Do = 0.7 mm). Comparison of model results (continuous lines) with experimental data of [11]

POB and COB evaporation

Once the model was validated, it was used to simulate the evaporation of POB and COB droplets at 0.1 MPa with an initial diameter of 0.7 mm and at 680 K, 700 K and 750 K. These temperatures were selected because they cover the range for which comparison between both biofuels is possible. Figure 7 shows that in a plot of normalized diameter vs. time, COB exhibits a lower evaporation rate than POB. This occurs because, according to Equation 5, for a constant environment temperature, the square diameter evolution in time depends only on fuel properties. The effect of thermal conductivity and heat capacity should be minor as both fuels exhibit similar values for these properties. Contrary, at the temperature selected, the density and latent heat of vaporization for COB are higher than those or POB which results in a lower slope and, therefore, a lower evaporation rate. The model reflects that stronger intermolecular forces between atoms, as those that exist in COB, contribute to a lower evaporation rate.

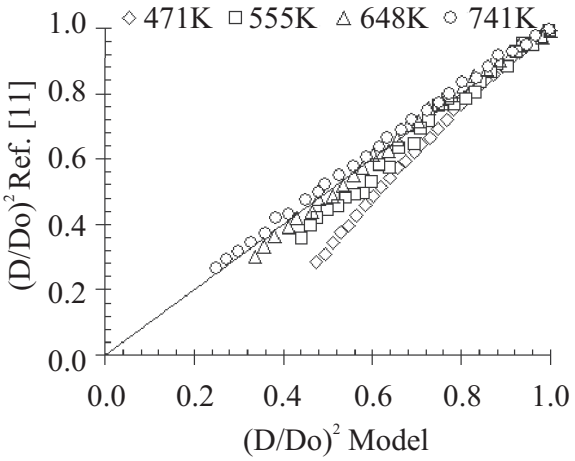

Figure 6 Parity plot for n-heptane dimensionless squared diameter. Experimental data of [11] vs. model predictions

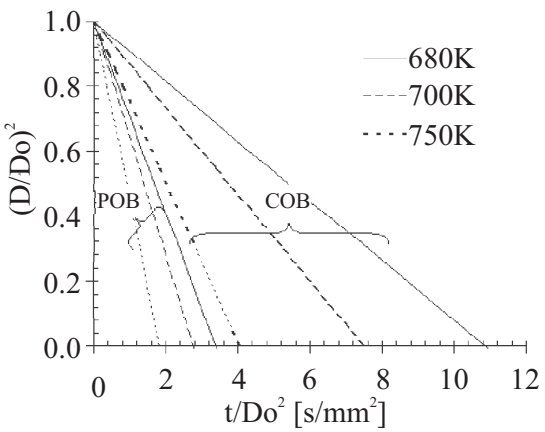

Figure 7 Variations of squared dimensionless droplet diameter with time divided by squared initial diameter of COB and POB according to D^2 law (Do = 0.7 mm)

A lower evaporation rate for COB could increase the ignition delay time for the fuel. Depending on engine design, these differences could favor particulate matter formation and decrease combustion efficiency. Adjustments on injection time that account for differences in evaporation rate, based on our model results, could help to avoid these problems.

Conclusions

A set of correlations carefully selected from the literature, based on chemical structure, group contribution and some physical properties of alkyl ester mixtures correctly predicts the physical and chemical properties required to model evaporation. While the values of density, vaporization enthalpy and heat capacity of castor oil are higher than those for palm oil, thermal conductivities have similar values. The reason for the trends is that density, vaporization enthalpy and heat capacity increase with chain length, unsaturation degree and concentration of hidroxyl groups. Contrary, thermal conductivity decreases as the degree of molecular unsaturation increases.

A model, based on D^2 law and successfully validated with experimental data found in literature for n-heptane shows that the evaporation rate of COB is lower than that of POB. The lower evaporation rate of COB occurs because of a high level of unsaturation and the presence of hydroxyl- groups on the main component of COB, methyl ricinoleate. Differences in evaporation rate between COB and POB may be important when optimizing the performance of biodiesel engines.

Acknowledgements

We acknowledge financial support from *Dirección Nacional de Investigación Medellín (DIME)*, *Universidad Nacional de Colombia, Sede Medellín* under Research project "*Modelo para la evaporación de gotas de biocombustible*", QUIPU code 20201007095. MLB is thankful to COLCIENCIAS and Universidad Nacional de Colombia for a *Jóvenes Investigadores* research grant. Authors are thankful to Professor Pedro Benjumea from Universidad Nacional de Colombia, Sede Medellín, for providing useful comments on this manuscript.

References

1. K. Bozvas. "Biodiesel as an alternative motor fuel: Production and policies in the European Union". *Renewable and Sustainable Energy Reviews*. Vol. 12. 2008. pp. 542-552.
2. M. Fangrui, A. H. Milford. "Biodiesel production: a review". *Bioresource Technology*. Vol. 70. 1999. pp. 1-15.
3. S. A. Basha, K. Gopal, S. Jebaraj. "A review on biodiesel production, combustion, emissions and performance". *Renewable and Sustainable Energy Reviews*. Vol. 13. 2008. pp. 1628-1634.
4. A. Murugesan, C. Umarani, R. Subramanian, N. Nedunchezhian. "Bio-diesel as an alternative fuel for diesel engines-A review". *Renewable and Sustainable Energy Reviews*. Vol. 13. 2009. pp. 653-662.
5. C. K. Law. *Combustion Physics*. Ed. Cambridge Press. New York. 2006. pp. 213-217.
6. W. A. Sirignano. "Fuel droplet vaporization and spray combustion theory". *Progress in Energy Combust Science*. Vol. 9. 1983. pp. 291-322.
7. J. B. Heywood. *Internal Combustion Engine Fundamentals*. Ed. McGraw Hill. México. 1988. pp. 491-502.
8. G. Castanet, P. Lavieille, F. Lemoine, M. Lebouché, A. Atthasit, Y. Biscos. "Energetic budget on an evaporating monodisperse droplet stream using combined optical methods Evaluation of the convective heat transfer". *International Journal of Heat and Mass Transfer*. Vol. 45. 2002. pp. 50-67.
9. C. Maqua, G. Castanet, F. Lemoine. "Bicomponent droplets evaporation: Temperature measurements and modelling". *Fuel*. Vol. 87. 2008. pp. 2932-2942.
10. C. Maqua, G. Castanet, F. Grisch, F. Lemoine, T. Kristyadi, S. S. Sazhin. "Monodisperse droplet heating and evaporation: Experimental study and modelling". *International Journal of Heat and Mass Transfer*. Vol. 48. 2008. pp. 3261-3275.
11. H. Nomura, H. Yasushige, H. J. Rath, S. Junichi, K. Michikata. "Experimental study on high-pressure droplet evaporation using microgravity

conditions". *Proc. Comb. Inst*. Vol. 26. 1996. pp. 1267-1273.

12. A. P. Kryukov, V. Levashov, Yu, S. S. Sazhin. "Evaporation of diesel fuel droplets: Kinetics versus hydrodynamic models". *International Journal of Heat and Mass Transfer*. Vol. 47. 2007. pp. 2541-9.

13. S. S. Sazhin, P. A. Krutitskii, W. A. Abdelghaffar, E. M. Sazhina, S. V. Mikhalovsky, S. T. Meikle, M. R. Heikal. "Transient heating of diesel fuel droplets". *International Journal of Heat and Mass Transfer*. Vol. 47. 2004. pp. 3327-2240.

14. S. S. Sazhin, W. A. Abdelghaffar, P. A. Krutitskii, E. M. Sazhina, M. R. Heikal. "New approaches to numerical modelling of droplet transient heating and evaporation". *International Journal of Heat and Mass Transfer*. Vol. 48. 2005. pp. 4215-28.

15. S. S. Sazhin, W. A. Abdelghaffar, M. R. Heikal. "Models for droplet transient heating: Effects on droplet evaporation, ignition, and break-up". *International Journal of Thermal Sciences*. Vol. 44. 2005. pp. 610-22.

16. S. S. Sazhin, T. Kristyadi, W. A. Abdelghaffar, M. R. Heikal. "Models for fuel droplet heating and evaporation: Comparative analysis". *Fuel*. Vol. 85. 2006. pp.1613-1630.

17. G. A. E. Godsave. "Studies of the combustion of drops in a fuel spray-the burning of single drops of fuel". *Proceedings of the Combustion Institute*. Vol. 4. 1953. pp. 818-30.

18. S. L. Manzello, M. Y. Choi, A. Kazakov, F. L. Dryer, R. Dobashi, T. Hiranothe. "Burning of large n-Heptane droplets in microgravity". *Proceedings of the Combustion Institute.* Vol. 28. 2002. pp.1079-1086.

19. S. R. Turns. *An introduction to combustion: Concepts and applications.* 2ª ed. Ed McGraw-Hill. New York. 2001. pp. 1613-30

20. D. B. Spalding. "The combustion of liquid fuels". *Proceedings of the Combustion Institute*. Vol. 4. 1953. pp. 847-64.

21. W. Yuan A. C. Hansen, Q. Zhang. "Predicting the physical properties of biodiesel for combustion modelling". *American Society of Agricultural Engineers*. Vol. 46. 2003. pp. 1487-1493.

22. G. Knothe. "Dependence of biodiesel fuel properties on the structure of fatty acid alkyl esters". *Fuel Processing Technology.* Vol. 86. 2005. pp. 1059-1070.

23. P. Benjumea, J. Agudelo, A. Agudelo. "Basic properties of palm oil biodiesel diesel blends". *Fuel*. Vol. 87. 2008. pp. 2069-2075.

24. R. C. Reid, J. M. Prausnitz, B. R. Poling. *Properties of gases and liquids*. 5ª ed. Ed. McGraw Hill. 1986. pp. 3.6-3.8, 4.35-4.38, 7.19-7.24,10.12.

25. R. E. Tate, K. C. Watts, C. A. W Allen, K. I. Wilkie. "The densities of three biodiesel fuels at temperatures up to 300ºC". *Fuel*. Vol. 85. 2006. pp. 1004-9.

26. J. Wei. *Product Engineering: Molecular Structure and Properties*. Ed. Oxford University Press. 2007. pp. 72-124.

27. G. W. Castellan. *Physical Chemistry.* 3ª. ed. Ed. Addison-Wesley Publishing Company. New York. 1983. pp. 85-90.

28. G. Waddington, S. S. Todd, H. M. Huffman. "An improved flow calorimeter. Experimental vapor heat capacities and heats of vaporization of n-heptane and 2,2,3-trimethylbutane". *Journal of the American Chemical Society.* Vol. 69. 1947. pp. 22-30.

29. Nist Chemistry Webbook. http://webbook.nist.gov/chemistry/. Consultada el 17 de abril de 2009.

30. D. Goodwin. Cantera, object-oriented software for reacting flows. http://www.cantera.org. Consultada el 20 abril de 2009.

31. B. J. McBride, S Gordon. *Computer program for calculation of complex chemical equilibrum compositions and applications*. "Lewis Research Center, National Aeronautics and Space Administration". Vol. 177. 1996.